ELSEVIER

Biophysical Chemistry 64 (1997) 175–197

Biophysical Chemistry

Thermodynamics of protein unfolding: questions pertinent to testing the validity of the two-state model

Maurice R. Eftink *, Roxana Ionescu

Department of Chemistry, University of Mississippi, University, MS 38677, USA

Received 24 July 1996; accepted 11 September 1996

Abstract

We discuss a number of questions pertaining to the analysis of data to extract thermodynamic parameters for the reversible unfolding of proteins. Simulations are presented to illustrate problems in trying to test the validity of the two-state model, vis-a-vis a more complicated unfolding model. A conceptual and practical problem is how to consider the unfolded state and how to relate the observed signal to this state. We discuss the idea that the unfolded state can be described as a single macrostate, comprising a distribution of microstates having different degrees of solvent-accessible surface area. We also discuss the possibilities and thermodynamic consequences of having more than one unfolded state and of having a denaturant which both stabilizes and destabilizes the protein's native state. © 1997 Elsevier Science B.V.

Keywords: Protein stability; Protein unfolding; Thermodynamics; Two-state model

1. Introduction

Thirty years ago Lumry et al. [1] published a notable paper on the validity of the two-state hypothesis of cooperative conformational changes in proteins. This paper has influenced the way that many researchers have approached the study of the thermodynamics of protein unfolding. Although the denaturation of proteins had been studied long before the mid-1960s (see the excellent historical overview of Dill [2]), the present day explosion of interest in this subject was probably not foreseen by the protein pioneers. Determining the stability of a protein to temperature and denaturants has become a routine laboratory practice and a vast assortment of natural and mutant proteins are the subject of such studies. As was pointed out by Lumry et al. [1] and a number of other early researchers [3–9], what is most remarkable about protein unfolding is the cooperative character. For many, if not most, small globular proteins, unfolding can be reversible and can appear to be nearly perfectly a two-state transition between a native, N, and an unfolded, U, state, with negligible population of any equilibrium intermediate. This property continues to attract interest, as researchers try to discover how Nature has solved the problem of acquiring a functional three-dimensional structure from a linear polymer made under the direction of the genetic code.

Since its inception, the Gibbs Conferences have been a retreat for those who take a decidedly thermodynamic view of the protein folding problem. As a

* Corresponding author.

PII S0301-4622(96)02237-5

contribution to this special issue, we present some reflections on contemporary questions related to reversible, cooperative transitions in proteins—essentially a revisit of the "two-state hypothesis" article of Lumry, Biltonen, and Brandts.

2. What are the native and unfolded states?

We seem to have an adequate understanding of the native state of a protein, using "state" in a thermodynamic sense. Although we do not have values for the standard free energies and enthalpies of formation or the standard molar entropies of proteins in solution at 298 K, we do have values for other thermodynamic quantities, including their molar volume and heat capacity, and it is easy to appreciate that native proteins should behave thermodynamically as large, highly organized molecules. We have got pictures. High-resolution structures are available for many proteins from crystallography and solution NMR. The latter studies, in particular, remind us that the native state has a certain degree of flexibility (e.g. about loop regions, side-chain rotations, etc.). Still, the native macrostate is usually considered to be a narrow ensemble of microstates, with each microstate having a similar folding pattern, but being slightly different in enthalpy (entropy, volume, heat capacity, etc.) as a result of small differences in the number of broken intramolecular non-covalent contacts, rotational isomers, extent of solvation, vibrational levels, etc.

The unfolded state, however, is more difficult to visualize. Dill and Shortle [10] have provided a lucid discussion of denatured states [1] of proteins. A widely accepted view is that an unfolded state approaches a random flight coil (from a hydrodynamic point of view), has a significant degree of side chain flexibility, and has a significant degree of solvent exposure of its side chains and its backbone. There is evidence that the high temperature-induced unfolded state of some proteins is more compact (i.e. has some residual secondary structure) than the urea, guanidine–HCl, or pH-induced unfolded states [11–14]. Whereas pH-induced unfolding usually leads to an expanded state, a partially collapsed state, known as the A state, can be induced in many proteins at very low pH and/or by the presence of certain anions [15,16]. The unfolded state produced by high concentrations of urea and guanidine–HCl is thought to be the most expanded, which may have to do with the mechanism by which these agents act (i.e. possibly by binding to the peptide bonds or side chains of unfolded state, and, at least in the case of guanidine–HCl, imparting a charge on the unfolded state) [7,8]. Nevertheless, there are reports that suggest the persistence of some residual structure in proteins unfolded in urea and guanidine–HCl [17,18].

What we stress at this time, echoing Lumry et al. [1] and Dill and Shortle [10], is that the unfolded state should be considered to be a distribution of microstates, and that this distribution is expected to be much broader than that of the native state.

3. State, structure, signal—which do we mean?

Equilibrium thermodynamics deals with states, of course, which are described by standard molar values (population averaged over the ensemble of microstates) for one or more of the functions of state, Gibbs free energy, G, (or the chemical potential, μ), enthalpy, H, entropy, S, and volume, V; i.e. thermodynamic quantities that we can place at some level on an energy (or enthalpy, entropy, volume) diagram. In practice we usually deal with changes in the level of these quantities for some reaction or first-order transition between one state and another. Whereas a thermodynamicist is really concerned with states, our chemical instincts lead us to try to associate a structure with a particular state and to try to describe the changes in inter- and intramolecular forces that account for transitions/reactions between one state and another, hence, chemical thermodynamics. The casual substitution of "state" and "structure" occurs very easily in our minds and usually does not lead to confusion. However, we have to realize that, with a few exceptions (volume,

[1] Whereas we prefer to use the term unfolded state, considering "denatured" to carry the possibility of meaning irreversible, Dill and Shortle prefer to use the general term "denatured" state, which can be divided into fully "unfolded" state and "compact denatured" states.

pressure, and heat capacity), we do not have "meters" for directly measuring thermodynamic quantities or mole fractions. Nor do we have "cameras" for directly visualizing the structure of molecules in solution. Instead we have to rely upon a variety of indirect signals, many of them based on some type of spectroscopy, to yield information about both the mole fraction of states and their structural characteristics.

The above paragraph may seem pedantic, but the concepts bear on the central question of "what is a state" from a practical point of view in the study of protein transitions. We will discuss various types of signals below, but basically there has to be some signal change for us to track a transition between two or more states. Regarding the state–structure–signal triad, experimentally determining when a change in state has occurred is not always easy. There can be changes in state and structure that a particular signal does not sense, and there can be signal changes that may or may not be due to a change in state or structure. Consider a few examples.

1. The binding of a specific ligand to a native protein can significantly alter the free energy (and enthalpy, entropy, volume) of a protein and most researchers would agree that a change in thermodynamic state has occurred upon forming a complex. However, a "structure camera", if such an instrument existed, might or might not show a perceptible change in the structure of the protein and a particular signal may or may not be changed by the binding process. If the ligand is a proton, which protonates a histidine residue, for example, this two-state protonation reaction may be tracked by monitoring the NMR chemical shift of the imidazole $\epsilon 1$ proton, but there may be an imperceptible change in the structure of the protein.
2. Consider the existence of cis and trans isomers about a proline residue in an unfolded protein. The two isomeric states will have nearly the same free energy, and, unless they are focused on to the particular proline, a "structure camera" and most signals would not be able to detect the presence of two different structures. Yet there is a large free-energy barrier between the cis and trans isomeric forms. In equilibrium studies the above situation may adequately be treated in terms of a single unfolded macrostate, but kinetics studies would require the consideration of two unfolded states.
3. Consider the coexistence of compact structures and fully expanded structures of an unfolded protein. Further assume these species to have nearly the same free energy, to be only slightly different in enthalpy, and to be rapidly interconverting. A snapshot taken by a "structure camera" should show different looking structures for the two species. Certain types of signals might be different for the collapsed and expanded structures, and the rate of chemical interconversion of the structures will determine whether certain signals (e.g. NMR resonances) are resolved for each structure or whether the signals are dynamically averaged. However, it is questionable as to whether one should consider such collapsed and expanded structures to be separate thermodynamic states, if, as assumed, they have similar free energy and enthalpy (so that a shift in population between the two structures will be gradual with change in temperature). In such a case, it seems more reasonable to consider the collapsed and expanded structures (plus structures in-between) to be microstates that compose a single unfolded macrostate.

The point is that there can be some confusion between states, structures, and signals. When considering the validity of the two-state or other models for a cooperative transition in a protein, we really should be talking about thermodynamic states.

4. What is the most appropriate reaction coordinate?

In visualizing the energy diagram for a first-order protein unfolding reaction, we must contrive some axis for the progress of the reaction. This may seem a trivial point, but we think that it can be of value to ask the above question, particularly when one is considering unfolding studies involving more than one perturbation axis. The mean end-to-end distance (of the C-terminus and N-terminus) is one possibility, so long as one is not concerned with a disulfide bridge containing protein. Another possibility is the number of intramolecular contacts within the un-

folded state. A reaction coordinate that seems to be useful is the solvent accessible surface area (SASA). The SASA can be calculated from the crystal structure of a native state and a computer-generated extended chain for the fully solvated, unfolded form of the protein [19,20] (see Creamer et al. [21] for a discussion of the validity of computationally generated SASAs). Most importantly, the SASA is related to the mechanism of action of various perturbants.

In recent years, correlations of thermodynamic parameters for proteins and model systems, along with information from the crystal structures of the proteins, have led to a set of relationships that provide a good description (and prediction) of the thermodynamics of protein unfolding based on the structure of the protein [22,23]. Briefly, correlations have been established between the heat capacity, C_p (or the heat capacity change, ΔC_p), and the solvent accessible surface area (SASA, in Å^2) (or ΔSASA, the change in SASA upon unfolding of a globular protein). Proportionality constants to relate ΔC_p and ΔSASA have been established for the solvation of polar and apolar groups. Second, for the thermal unfolding of a protein, a correlation has been found between the value of its ΔC_p and the enthalpy change, ΔH_{un}, for the reaction; this correlation is based on the finding that there is a common temperature, T_H, of about 110 °C, at which there is a convergence of the ΔH_{un} for a large number of proteins. Likewise, there is a correlation between the value of ΔC_p and the component of the entropy change that can be related to solvation effects, ΔS_{solv}. The total entropy change, ΔS_{un}, must contain contributions from both solvation changes and changes in the configurational entropy, ΔS_{conf}, of the polypeptide backbone and side chains upon unfolding (i.e. $\Delta S_{un} = \Delta S_{solv} + \Delta S_{conf}$, where ΔS_{conf} can also be considered to be the entropy change for unfolding in the absence of solvent). The value of ΔS_{conf} can be estimated from computational analysis of the probability of side-chain rotamers and the chain entropy of the backbone [24–26]. Freire and coworkers [22,27,28] have had good success in exploiting this correlation between ΔSASA and ΔC_p to calculate ΔH_{un}, ΔS_{un}, and hence ΔG_{un} for the unfolding of globular proteins.

ΔSASA is also a very useful reaction coordinate for the consideration of protein unfolding reactions induced by other perturbants. Tanford [7,8] and Schellman [29] have argued that the ability of agents such as urea and guanidine–HCl to induce the unfolding of proteins is related to the change in the exposure of residues on unfolding and their favorable solvation by the chaotropic agent. Myers et al. [30] have shown that there is a good correlation between ΔSASA and the m values for urea and guanidine–HCl-induced unfolding of proteins. Pressure-induced unfolding of proteins has received less attention. Simply put, the application of pressure shifts the protein to a state with smaller volume, which may result in unfolding of the protein and/or subunit dissociation. The molecular explanation for the contributions to the volume change on unfolding are not certain. One explanation is that the negative ΔV for unfolding is due largely to contributions from the increase in density of water as it solvates newly exposed charged residues and apolar side chains of the unfolded state. Finally, pH-induced unfolding has been rationalized in terms of the existence of perturbed side-chain pK_a values in the native state, which are normalized when the protein unfolds, with the concomitant exposure and solvation of these ionizing groups. Whereas the pH-induced unfolding of a protein may, in some cases, be assigned to the existence of just a few such groups with perturbed pK_a values, the use of ΔSASA seems appropriate in this case as well, since the increase in accessibility of side chains results in normalization of their pK_a values.

5. What are the appropriate relationships to describe transitions along different perturbation axes (and do we all agree)?

Whereas temperature is an experimentally convenient perturbation with which to unfold proteins, many proteins do not show reversibility with respect to thermal unfolding, due, most likely to aggregation of the unfolded state, chemical reactions involving side chains at the elevated temperature, etc. Consequently, many studies of protein unfolding employ chemical denaturants or acid/base to induce unfolding reactions. Besides being alternative perturbation axes and being amenable to room temperature (thus minimizing irreversible reactions), the unfolding by

these latter agents provides additional ways to try to gain insights about protein stability. High pressure also can be used, although it requires specialized equipment.

An obvious issue, then, is whether there is agreement about the fundamental relationships to use to describe unfolding reactions (assumed to be two-state processes at this juncture) induced by traveling along the various perturbation axes. For thermal unfolding, a form of the Gibbs–Helmholtz equation (Eq. (1)) (all equations given in Table 1) is well established for the temperature dependence of the standard free energy change, $\Delta G_{un}(T)$, for the N $\rightleftharpoons$ U transition [31–33]. By definition, ΔH°_{un} and ΔS°_{un} are the standard enthalpy change and entropy change, respectively, for the conformational transition at the reference temperature, T°. If ΔC_p is positive, this relationship describes a parabolic curve of $\Delta G_{un}(T)$ versus T, with $\Delta G_{un}(T)$ being zero at both a high-temperature unfolding temperature, T_G, and at a low-temperature unfolding temperature, $T_{G'}$ (i.e. cold unfolding). Arguments have been made that the ΔC_p for protein unfolding may change with temperature, but within the experimental limits of most studies it appears that ΔC_p is constant [31,34].

For urea or guanidine–HCl-induced unfolding, there has been a good deal of discussion regarding the appropriate relationships. The most frequently

Table 1
Relationships describing the unfolding transitions in proteins

Temperature		
$\Delta G_{un}(T) = \Delta H^{\circ}_{un} + \Delta C_p \cdot (T - T^{\circ}) - T \cdot [\Delta S^{\circ}_{un} + \Delta C_p \cdot \ln(T/T^{\circ})]$	where ΔH°_{un} is the enthalpy change at $T = T^{\circ}$ ΔS^{0}_{un} is the entropy change at $T = T^{\circ}$ ΔC_p is the change in heat capacity upon unfolding	(1)
Chemical Denaturants		
$\Delta G_{un}([\mathbf{d}]) = \Delta G^{\circ}_{un} - m \cdot [\mathbf{d}]$	*Linear extrapolation model* ΔG°_{un} is the free energy change in the absence of **d** $m = \delta \Delta G_{un}/\delta[\mathbf{d}]$	(2)
$\Delta G_{un}([\mathbf{d}]) = \Delta G^{\circ}_{un} - \Delta n \cdot R \cdot T \cdot \ln(1 + K \cdot a_{\mathbf{d}})$	*Denaturant binding model* where $a_{\mathbf{d}}$ is the activity of **d** Δn is the change in number of **d** binding sites upon unfolding K is average (or equivalent) association constant for **d** to both N and U states	(3)
$\Delta G_{un}([\mathbf{d}]) = \Delta G^{\circ}_{un} + \Delta \alpha \cdot \Sigma n_i \cdot \delta g_{i,\text{transfer}}$	*Free energy of transfer model* $\Delta \alpha$ is the average change in solvent exposure of all protein side chains n_i is the number of amino acid side chains in the protein of type i $\delta g_{i,\text{transfer}}$ is free energy of transfer of side chain from water to denaturant solution	(4)
$\Delta G_{un}([\mathbf{d}]) = \Delta G^{\circ}_{un} + n \cdot \Delta G_{s,m} \cdot [\mathbf{d}]/(K_{den} + [\mathbf{d}])$	*Variation of transfer model* n is the total number of internal side chains $\Delta G_{s,m}$ is the maximum solvation energy at $[\mathbf{d}] \rightarrow \infty$, where ΔG_s is determined by averaging the $\delta g_{i,\text{transfer}}$ for the internal residues K_{den} is "denaturant constant", equal to [**d**], needed to achieve $\Delta G_{s,m}/2$	(5)
pH (equation given for H^+-induced unfolding)		
$\Delta G_{un}(\text{pH}) = \Delta G^{\circ}_{un} - RT \cdot \ln[(1 + [H^+]/K_{a,U})^n/(1 + [H^+]/K_{a,N})^n]$	$K_{a,U}$, $K_{a,N}$ are acid dissociation constants for groups on the U and N states n is number of groups (assumed to be equivalent) whose protonation is coupled to unfolding	(6)
$\Delta G_{un}(\text{pH}) = \Delta G^{\circ}_{un} - RT \cdot \ln[(1 + [H^+]/K_{a,U})^n$		(7)
Pressure		
$\Delta G_{un}(P) = \Delta G^{\circ}_{un} - \Delta V_{un} \cdot (P^{\circ} - P)$	ΔV_{un} is volume change for the N $\rightleftharpoons$ U transition P° is reference pressure	(8)

For a two-state transition, the mole fraction of the N and U states are given as $X_N = 1/Q$, $X_U = \exp(-\Delta G_{un}/RT)/Q$, where $Q = 1 + \exp(-\Delta G_{un}/RT)$ and the function for ΔG_{un} is taken from above; the average signal, $\langle \alpha \rangle_{calc} = \Sigma X_i \cdot (\alpha_i + x \cdot \delta \alpha_i/\delta x)$, where x is a generalized perturbant.

used relationship (Eq. (2)) is associated with the so-called linear extrapolation model (LEM). In this equation ΔG°_{un} is the free-energy change for the unfolding transition in the absence of denaturant, **d** (at reference conditions of T, pH, etc., designated by °), and $m = \delta\Delta G_{un}/\delta[\mathbf{d}]$ is the dependence (assumed to be linear, hence the name of the model) of ΔG_{un} on denaturant concentration. Though simple and empirical, this relationship has been found to adequately describe unfolding data in a number of cases [35–38]. The value of m is thought to be directly proportional to the change in solvent accessible surface area upon unfolding [29]. Two alternatives to this model are the denaturant binding model [8,38–40], which assumes that the denaturant has a weak, average association constant, K, for protein residues and that there is a change in the number of accessible binding sites, Δn, upon unfolding, and the free energy of transfer model [8,38], which uses experimentally determined free energies of transfer, $\delta g_{transfer,i}$, for the amino acid side chain from water to the denaturant solution and assumes that there is an average change in solvent exposure, $\Delta\alpha$, of the n amino acid residues upon unfolding. Both of these models have merit, but they involve extra thermodynamic terms (the average K or $\Sigma\delta g_{transfer,i}$ for all the amino acids). Direct evidence that urea and guanidine–HCl bind to both native and unfolded states of proteins provides strong support for the binding model [40]. A variation of the transfer model has been presented by Staniforth et al. [41], which includes both an empirical, average partition constant for the transfer of amino acid side chains from water into the denaturing solution and a maximum solvation energy change, $\Delta G^{\circ}_{s,m}$, along with the number of internal side chains that become exposed, n. A prediction of the binding model, free energy of transfer model, and the latter model of Staniforth et al. is that the plots of ΔG_{un} versus **[d]** may be non-linear, especially for guanidine–HCl, as has been observed in some cases [42,43]. It can be seen from Eqs. (2) and (5), that $m = n \cdot \Delta G_{s,m}/(K_{den} + [\mathbf{d}])$; thus m will be larger at lower **[d]**. This dependence of m on **[d]** may account for the variation of m with $[\mathbf{d}]_{1/2}$ that is sometimes seen in studies with a large set of mutant proteins. Despite the evidence for denaturant binding and a non-linear dependence of ΔG_{un} on **[d]**, the LEM model still is popular, due, no doubt, to its simplicity and to the fact that the above-mentioned deviations from linearity are small for urea.

pH-induced unfolding of proteins would seem to offer the advantage that there are relatively few, discrete binding sites (i.e. protonation sites) for the perturbant. However, this apparent simplicity can be misleading. To have a concerted unfolding induced by protons (or hydroxide ions), there must be several groups on the protein with perturbed pK_a values, which all become protonated (or deprotonated) upon a two-state unfolding transition of the protein. For the low pH-induced unfolding of a protein, Eq. (6) can apply, where $K_{a,U}$ and $K_{a,N}$ are the acid dissociation constants for the n groups on the protein in the unfolded and native states, respectively. ΔG°_{un} in this case is specifically defined to be the free energy change for the unfolding of the unprotonated N state to the unprotonated U state; in other equations in Table 1, the ΔG°_{un} value may depend on the pH. This model implicitly assumes that all n groups have the same K_a value in a particular state, a fairly generous assumption. This relationship is often simplified further by assuming that the $K_{a,N}$ of the groups in the native state is very large (i.e. that the groups do not become protonated in the native state). The relationship then becomes Eq. (7). This type of model actually works well in describing the pH-induced unfolding of several proteins, but one can imagine that cases should exist in which the n groups are not equivalent in their $K_{a,U}$ values (i.e. a combination of Asp, Glu, and His residues with perturbed K_a values) or cases in which some residues have their K_a largely perturbed (Eq. (7)) while some have their K_a perturbed to a lesser degree (Eq. (6)).

For pressure-induced unfolding reactions, Eq. (8) is commonly used, where P^0 is the reference pressure (usually 1 atm) and where ΔV_{un} is the difference in volume of the final and initial states, which includes (and may be dominated by) solvation effects. It is not so clear whether or not ΔV_{un} is a constant or depends on pressure or other conditions, such as temperature or denaturant concentration, etc. Early studies suggested a negative value for the change in compressibility, $\Delta\beta$ $(= \delta\Delta V_{un}/\delta P)$, and a positive value for the change in thermal expansivity, $\Delta\alpha$ $(= \delta\Delta V_{un}/\delta T)$, for pressure-induced unfolding [44,45], but more recent studies seem to show these terms to be small [46,47]. Of course, the

values of $\Delta\beta$ and $\Delta\alpha$ may vary from protein to protein and more systematic studies are necessary.

6. Two-state or not two-state?

When studying the stability of a protein, a primary question is whether the unfolding transition, induced by temperature, denaturants, pH, etc., is described by a two-state model ($N \rightleftharpoons U$) or a more complicated multi-state model (i.e., $N \rightleftharpoons I_1 \rightleftharpoons I_2 \cdots U$, where I_i are equilibrium folding intermediates) [2]. Deciding upon an unfolding model is of paramount importance, for the evaluation of thermodynamic quantities is model dependent and the model provides the context for drawing molecular interpretations. The Occam's razor approach is to assume the transition to be two-state until the data indicate otherwise.

Lumry et al. described tests of data for the validity of the two-state model for a conformational transition of a protein. One test is to determine whether the van't Hoff enthalpy change, ΔH_{vH}, is constant throughout a transition or goes through a maximum near the apparent midpoint of the transition. If the latter occurs, this indicates a multi-state process. This rather intricate sounding test really amounts to determining the degree to which the data are fitted by the functional shape of a two-state process. A second test, which is increasingly used, is to monitor an unfolding transition by two or more independent observable quantities. If such different data sets do not provide an identical tracking of the progress of the transition (after properly taking into account differences in pre- and post-transition baseline slopes), this is an indication that the process is multi-state. The converse argument, that identical trackings indicates a two-state process, is not rigorously true (since it is possible for two observable quantities both to be insensitive to one or more transitions in a multi-step process). However, the chance of such coincidences decreases with the use of three or more observable quantities and this test provides a convenient means to try to determine the appropriate unfolding model (two-state or otherwise). This is especially true with the use of "multi-dimensional" instruments that can monitor two or more types of signals (e.g. fluorescence and circular dichroism) on the same sample (to avoid sample-to-sample variations), combined with the use of global non-linear least-squares analysis [48,49]. Also, this "multiple observable" test is amenable to transitions induced by perturbants other than temperature. A third test of the two-state model is to compare the calorimetrically determined enthalpy change, ΔH_{cal}, with the van't Hoff enthalpy change, ΔH_{vH}, determined for the same process. With modern scanning calorimeters the latter ΔH_{vH} can be determined by fitting the two-state model to excess heat capacity data. If the ratio $\Delta H_{vH}/\Delta H_{cal}$ is equal to unity, this confirms that the transition is two state. Ratios less than one indicate a multi-state process.

7. How do different types of signals track a conformational transition?

Essentially one has to know one's method. Along with scanning calorimetry, spectroscopic methods are most commonly used to study unfolding transitions. There are two important types of such spectroscopic measurements (see Fig. 1). One type of measurement is that in which the measured signal, $\langle\alpha\rangle$, is a mole fraction weighted average over the signals of the components in the system. The other type of useful measurement is that which can give a discrete, resolved signal for the native and/or unfolded state. For both types the signal must be linearly related to the concentration of species in solution. Methods can also be categorized as to whether they sense overall changes in the radius, shape, or secondary structure of a protein or whether they probe changes in the local microenvironment of individual side chains. Our emphasis here is on the first type of categorization and how mole fractions can be determined from the signals.

The weighted average signals (Fig. 1(A)) include such measurements as steady-state fluorescence, circular dichroism, absorbance, Fourier transform in-

[2] We do not want to enter the discussion about second-order transitions. We will discuss several types of perturbation axes, not just temperature, for which a second-order transition can be defined. Instead, we will present simulations for multi-state transitions and a distribution of unfolded states, as possible phenomena that might be something like a second-order transition.

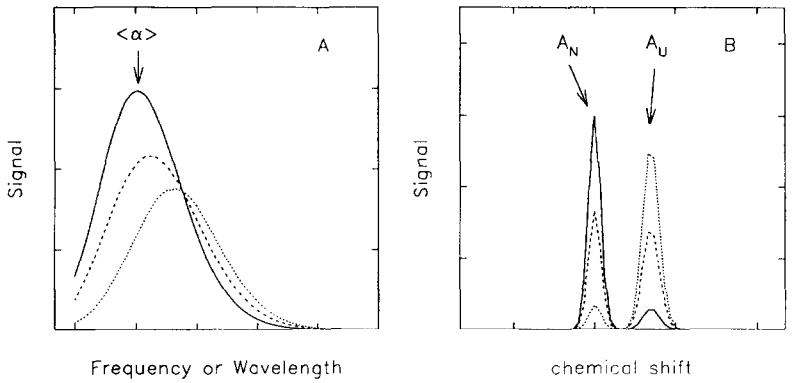

Fig. 1. (A) Simulated mole fraction weighted spectral data for a two-state system. The value of the signal, $\langle \alpha \rangle$, (e.g. steady-state fluorescence intensity) can be monitored at some frequency/wavelength as a function of the perturbation axis. Shown in the simulation are mixtures with $X_N = 0.9$, $X_U = 0.1$ (————); $X_N = 0.5$, $X_U = 0.5$ (— — —); and $X_N = 0.1$ and $X_U = 0.9$ (- - -). Notice that an isosbestic (or isoemissive or isodichroic) point that can be found at some frequency if there are only two interconverting states and if the spectra cross. (B) Simulated resolved signals (e.g. NMR resonances) for a two-state system. The integrated area of either peak should track the transition.

frared (FTIR) spectroscopy, and excess heat capacity. These types of signals are averages because the methods are not able to separately resolve signals from the native and unfolded states. The average signal (at any particular experimental conditions, such as wavelength) is related to the mole fraction of species via $\langle \alpha \rangle = \Sigma X_i \alpha_i$, where X_i is the mole fraction of state i and α_i is the intrinsic signal of the pure i state (at the particular experimental conditions; see following discussion of baseline slopes). If one induces a transition by varying temperature, **[d]**, pH, etc., the resulting variation in X_i should be describable by the appropriate thermodynamic model and parameters (e.g. non-linear least-squares fitting of $\langle \alpha \rangle_{exp}$ versus perturbant data with the equation $\langle \alpha \rangle_{calc} = \Sigma X_i \cdot \alpha_i$, where the X_i values are related to ΔG_{un} and the perturbation axis by one of the equations in Table 1; see Ref. [50] for the full forms of several of these equations, including the baseline slopes discussed below).

In addition to there being a difference in signal between the N and U states, it is important to realize that the intrinsic signals for the N and U (and other) states may also depend on the perturbation axis, giving sloping pre-transition and post-transition baselines. That is, the α_i for the individual states may depend on temperature, **[d]**, etc (i.e. non-zero terms for $\delta\alpha_i/\delta x$, where x is the extent of perturbation). Consequently, α_U may appear to be different if U is formed by traveling along different perturbation axes and such differences, if observed, will not necessarily mean that different U states have been formed. This can complicate the fitting of data and this is where knowing the limitations of the data are important. As an example of baseline slopes, the steady-state fluorescence intensity of tryptophan (the most commonly used intrinsic fluorophore for studying unfolding transitions) or any fluorophore in water will decrease with increasing temperature, with a functional dependence that is well established [50,51]. Although this decrease of fluorescence with temperature is non-linear, it is usually satisfactory to assume a linear dependence, within any temperature range of about 30°. Typically, the fluorescence of fluorophores in an apolar microenvironment (e.g. buried in a native protein) will show a smaller temperature dependence than a fluorophore in an aqueous microenvironment (e.g. in an unfolded protein). A couple of advantages of using fluorescence to monitor temperature-induced transitions is that it is safe to assign any increase in signal, with increasing temperature, to a conformational transition, since thermal quenching will always decrease the baseline signals, and fluorescence provides some structural selectivity, in that it focuses specifically on changes in the environment of the fluorophores (i.e. tryptophan residues). The fluorescence of *N*-acetyl tryptophanamide (NATA) is also known to increase, al-

most linearly, with increasing concentrations of urea or guanidine–HCl [50,52]. H^+ and OH^- ions quench the fluorescence of tryptophan and NATA in a Stern–Volmer manner; this may need to be considered below pH 3 and above pH 11, since the quenching constants for both ions is on the order of 20 M^{-1} [53]. The protonation of histidine residues, in either the native or unfolded state of proteins, makes them better quenchers of tryptophan fluorescence [54,55]; this is a basis for a fluorescence change that may be unrelated to a conformational transition.

Far-UV CD signals sense changes in secondary structure, primarily α-helix content, throughout a protein. For helical proteins, CD signals at 222 nm are known to vary slightly with temperature [56]. CD signals also usually show small and fairly linear baseline slopes with the addition of urea or guanidine–HCl, and whether or not the slopes are ascending or descending may depend on wavelength [57,58]. Difference absorbance measurements in the aromatic region for both native and unfolded states can depend on temperature and denaturant concentrations. For temperature, such baseline variations are small and are probably due to a combination of changes in refractive index and changes in concentration due to thermal expansion of the solution [52]. Thus, for each of these optical signals, the "baseline" regions in a plot of $\langle \alpha \rangle$ versus perturbant can be significant and should be included as fitting parameters in a non-linear least-squares analysis. For fitting the equations in Table 1 to data [3] one should use non-linear least-squares or another fitting routine in order to avoid the human factor when drawing baselines.

Resolved signals (Fig. 1(B)) are possible with NMR (in the slow exchange limit) and can sometimes be achieved with certain other methods such as time-resolved fluorescence. What is key with such methods is the ability to resolve a signal, say a NMR peak, for a particular conformational state of the protein. The variation of the amplitude (or the integrated area of a peak or cross peak) of the signal, A_i, with variation of the perturbant then provides a direct tracking of the population of state i during the transition [60–62]. Further, if one can assign several NMR peaks to particular aromatic residues, for example, and monitor these amplitudes as a function of perturbant, this provides a "multiple observable" test of the two-state model. Huang and Oas [63] have recently used this strategy by simultaneously monitoring changes in the chemical shift of four aromatic residues in a λ repressor and have showed that coincident two-state thermal unfolding is observed for each resolved signal under all conditions studied. It is also important to note that with NMR signals there can be a dynamic averaging of resonances, if the frequency of chemical interconversion between species is faster than the difference (absolute value of) in NMR frequencies of the resonances of the two forms. In the rapid exchange regime, one will not observe resolved signals for each state, but the position (chemical shift) of the resonance will be an average of that for the two states and can be analyzed like signals in the first category.

The pre-exponential factors associated with fluorescence lifetime components can be used, like the amplitudes of NMR peaks, to track the population of species [64,65]. In time-resolved fluorescence energy transfer studies, it is likewise possible, in some cases, to analyze the data in terms of a bimodal distribution of donor-to-acceptor distances, with the amplitude of each component being related to the population of a conformational state [66].

Among other methods, capillary electrophoresis [67,68] and size-exclusion chromatography [69–71] have the potential for physically separating N and U species, if they interconvert more slowly than they migrate through a capillary or column. If interconversion is rapid, a mole fraction averaged electrophoresing or eluting peak will be obtained for these methods as well as for urea gradient gel electrophoresis [72]. FTIR signals generally give unresolved, averaged signals for the vibrational absorbances of proteins in solution. There can be some partial resolution of peaks, particularly for the amide stretching assigned to β-sheet and the ring vibration of tyrosine residues; tracking the change in signal at different regions of the FTIR spectrum thus can be used as a "multiple observable" test of the thermal unfolding of proteins [73,74]. Small-angle X-ray scattering (SAXS) data can provide information about the radius of gyration and the shape of a protein in

[3] Compiled programs for fitting Eqs. (1), (2), (7) and (8) to data, including global analyses, will be provided upon request. These programs are based on Johnson's NONLIN [59].

solution and this method is beginning to be used to study structural transitions of proteins as a function of some perturbation axis [75,76].

8. Again the question: two-state or not two-state? If not two-state, then what?

If one of the above experimental tests leads to doubt regarding the two-state model, then what is next? The next most logical model is the three-state model, $N \rightleftharpoons I \rightleftharpoons U$, where I is an equilibrium folding intermediate. Actually, the distinction between the two- and three-state models is a matter of degree; the population of intermediate states is considered to be undetectably small for a two-state model. The ability to distinguish between these models rests not only on the population of the intermediate state but also on the signal being monitored, as simulations below will show. If, for example, the fluorescence signal of an I state is much larger than that of either the N or U states, the existence of a small mole fraction of the I state will be easier to determine, thus revealing the three-state behavior.

Progressing from the three-state model, we consider a multi-state transition, $N \rightleftharpoons U_1 \rightleftharpoons U_2 \rightleftharpoons U_3 \rightleftharpoons U_4$ [4]. A model with this many states is not tractable for data fitting, but it is useful to show simulations of the expected patterns for unfolding transitions for a two-state, three-state, and five-state transition. For the five-state transition, we also consider two possibilities; one case is that in which the free energy levels for the states are equally spaced; the second case is that in which the free energy levels are asymmetrically spaced, with the $N \rightleftharpoons U_1$ step having the largest ΔG°. In the simulations that follow we consider each individual step to be a two-state process (i.e a three-state transition is a sequence of two two-state processes) and we consider each state to be a discrete thermodynamic macrostate. In a following section we will illustrate the patterns when the U state is a distribution of microstates.

Shown in Fig. 2 are simulated patterns for the denaturant-induced transitions in which some weighted average signal, $\langle \alpha \rangle$, is monitored. The sigmoidal dashed curves in each panel are for a two-state transition between N with $\alpha_N = 1$ and U with $\alpha_U = 0.2$ ($\Delta G^\circ_{un} = 5$ kcal mol^{-1} and $m = 5$ kcal mol^{-1} M^{-1}). For each simulation, the $\Sigma \Delta G^\circ_{un,i}$ and Σm_i are also 5 kcal. The labelled horizontal lines in each panel show the assumed relative free-energy levels for the states (i.e. how the 5 kcal is split between the steps) in the absence of perturbant. Eq. (2) is used to simulate the effect of the denaturant. In simulating the data, we have assumed baseline slopes for the pure states to be zero (i.e. $\delta\alpha_N/\delta[\mathbf{d}] = \delta\alpha_U/\delta[\mathbf{d}] = 0$) for simplicity and no random error has been added. The "data" were then fitted via non-linear least-squares (solid lines) to a two-state model to see how well such an incorrect model would fit and recover the apparent thermodynamic parameters.

For the symmetrical three-state (panel A) and symmetrical five-state (panel B) transitions, we first have assumed that there are equal step-wise variations in the values of $\Delta G^\circ_{un,i}$, m_i, and signal (i.e. $\Delta G^\circ_{un,i}$ and m_i of 2.5 kcal for $N \rightleftharpoons I$ and $I \rightleftharpoons U$, with $\alpha_N = 1$, $\alpha_I = 0.6$, and $\alpha_U = 0.2$ for the three-state process; the $\Delta G^\circ_{un,i}$ and m_i values all being 1.25 kcal, with $\alpha_N = 1$, $\alpha_{U1} = 0.5$, $\alpha_{U2} = 0.4$, $\alpha_{U3} = 0.3$, and $\alpha_{U4} = 0.2$ for the five-state process). As shown in Fig. 2(A) and 2(B), these symmetrical three-state and five-state transitions are sigmoidal and are fitted very well by a two-state model (solid lines). The transitions become increasingly broad with increasing number of states, and the apparent (i.e. fitted to a two-state model) ΔG°_{un} and m' become progressively lower than the input $\Sigma \Delta G^\circ_{un,i}$ and Σm_i of 5 kcal each. Such symmetric transitions will not be distinguishable from an actual two-state transition. As will be shown below, for a three-state transition to be determinable, there must be some asymmetry in the thermodynamic parameters and/or the signal changes for the steps. Before showing more detailed simulations with the three-state model, consider a

[4] This represents a series of first-order transitions; five states being enough to illustrate the behavior. Note that the U_1, U_2, and U_3 species could be considered to be intermediates, I_1, I_2, and I_3 if these species have some compactness, for example, if the stepwise process involves unfolding of multiple sub-domains of a protein. Also note that the sequential representation for the transitions is just a matter of convenience for simulating the thermodynamics of the system and does not preclude transitions between N and any of the U states, with a ΔG_{un} value that is additively related to the other values.

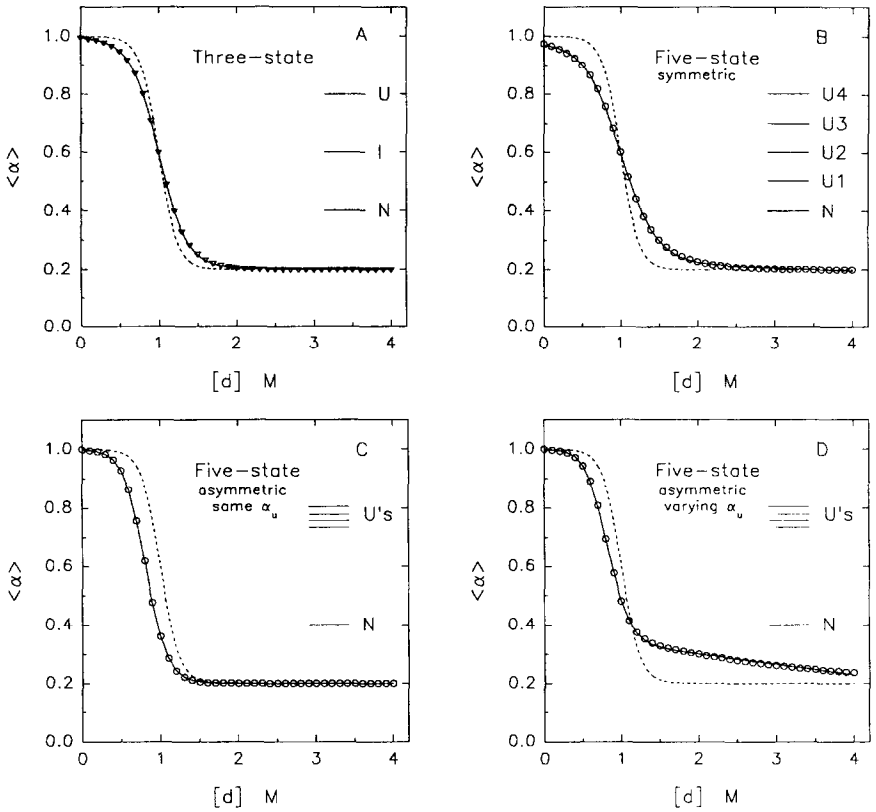

Fig. 2. Simulated transition data, $\langle \alpha \rangle$ versus **[d]**, for the following models. The α_N of the native state is assumed to be 1.0; the α_U of the final unfolded state is assumed to be 0.2; pre- and post-transition baselines are assumed to be zero. The free-energy diagrams for the models are given as insets in the panels. In each case the sum of the $\Delta G^{\circ}_{un,i}$ values is 5.0 kcal mol^{-1} and the sum of the m_i values is 5.0 kcal mol^{-1} M^{-1}. The dashed line in each case is a simulation for a two-state transition with ΔG°_{un} = 5.0 kcal mol^{-1} and m = 5.0 kcal mol^{-1} M^{-1}, for comparison. The solid lines are the best fit of a two-state model to the simulated multi-state "data". (A) Symmetrical three-state model, with $\Delta G^{\circ}_{un,1} = \Delta G^{\circ}_{un,2}$ = 2.5 kcal mol^{-1}, $m_1 = m_2$ = 2.5 kcal mol^{-1} M^{-1}, and α_I = 0.6. The fit is with $\Delta G^{\circ\prime}_{un}$ = 3.32 kcal mol^{-1} and m' = 3.31 kcal mol^{-1} M^{-1}. (B) Symmetrical five-state model, with $\Delta G^{\circ}_{un,1} = \Delta G^{\circ}_{un,2} = \Delta G^{\circ}_{un,3} = \Delta G^{\circ}_{un,4}$ = 1.25 kcal mol^{-1}, $m_1 = m_2 = m_3 = m_4$ = 1.25 kcal mol^{-1} M^{-1}, α_{U1} = 0.8, α_{U2} = 0.6, α_{U3} = 0.4, and α_{U4} = 0.2. The fit is with $\Delta G^{\circ\prime}_{un}$ = 2.51 kcal mol^{-1} and m' = 2.52 kcal mol^{-1} M^{-1}. (C) Asymmetrical five-state model, with $\Delta G^{\circ}_{un,1}$ = 4.0 kcal mol^{-1}, $\Delta G^{\circ}_{un,2} = \Delta G^{\circ}_{un,3} = \Delta G^{\circ}_{un,4}$ = 0.33 kcal mol^{-1}, m_1 = 4.0 kcal mol^{-1} M^{-1}, $m_2 = m_3 = m_4$ = 0.33 kcal mol^{-1} M^{-1}, and $\alpha_{U1} = \alpha_{U2} = \alpha_{U3} = \alpha_{U4}$ = 0.2. The fit is with $\Delta G^{\circ\prime}_{un}$ = 3.55 kcal mol^{-1} and m' = 4.36 kcal mol^{-1} M^{-1}. (D) Asymmetrical five-state model, with above thermodynamic parameters and α_{U1} = 0.5, α_{U2} = 0.4, α_{U3} = 0.3, and α_{U4} = 0.2. The fit is with $\Delta G^{\circ\prime}_{un}$ = 3.33 kcal mol^{-1} and m' = 4.09 kcal mol^{-1} M^{-1}.

couple of additional aspects of the five-state model. Fig. 2(C) and 2(D) show simulations for asymmetric transitions in which the first step has a large ΔG°_{un} and m, and the subsequent steps are smaller and thus are not as sharp along the **[d]** axis. This type of asymmetric five-state model may be relevant to actual protein systems, where it is suspected that the initial unfolded state can undergo further weakly cooperative transitions as additional denaturant is added (or as other conditions are varied). Fig. 2(C) is a simulation for the case in which all the signal change occurs in the first $N \rightleftharpoons U_1$ step, with no incremental signal change on going from the U_1 to U_4 states. The resulting plot of $\langle \alpha \rangle$ vs. **[d]** can be fitted very well to a two-state model with an apparent $\Delta G^{\circ\prime}_{un}$ that is about 90% (3.55 kcal mol^{-1}) of the input value (4 kcal mol^{-1}) for the $N \rightleftharpoons U_1$ step. The apparent m' is actually larger (4.36 kcal mol^{-1} M^{-1}) than the input value for the first step (4 kcal mol^{-1} M^{-1}). Fig. 2(D) is a simulation for the case

where the signal of the U states progressively decreases. The sloping final baseline is due both to this incremental variation in the signals and to the gradual shift from U_1 to U_4 states with increasing [**d**]. This plot can also be fitted very well by the two-state model with a final sloping baseline. The apparent ΔG°_{un} is about 83% of the input value for the first step and the apparent m' is essentially the same as the input value.

The observation that a multi-state system can be well described by a two-state model illustrates a major difficulty in analyzing equilibrium unfolding data. Still there are a number of cases in which experimental results have clearly shown the need for a three-state model. For data to reveal the need for a three-state model (which is to say, that a two-state model is not adequate): (1) the amplitude of the intermediate state must be either higher or lower than that of both the N and U states, and/or (2) the maximum population of the I state must be sufficiently high. These two conditions are interrelated, so all we can do is show a few simulations. Fig. 3(A) shows simulations of the three-state model (symmetrical in thermodynamic steps, with $\Delta G^{\circ}_{un,1} = \Delta G^{\circ}_{un,2}$ and $m_1 = m_2$) in which the value of the signal for the intermediate is permitted to vary form values either above or below that of the N and U states. When α_I is anywhere between α_N and α_U, the data can be well fitted by a two-state model, yielding apparent values of ΔG°_{un} and m' that are lower than the $\Sigma\Delta G^{\circ}_{un,i}$ and Σm_i. When α_I is either much larger or much lower than α_N or α_U, the deviation from a two-state fit (solid lines) is evident. The dashed curve in Fig. 3(B) is the sum of the square of the residuals (SSR) for the two-state fit; when the value of SSR is greater than about 0.04, the inadequacy of the two-state fit can be seen in these simulations (of course, the ability to make this judgement for real experiments will depend on the standard deviations of the data). Also shown in Fig. 3(B) is a plot of recovered apparent ΔG°_{un} and m' values as a function of α_I, with a horizontal line drawn at 5.0 kcal mol^{-1} for comparison (which is the value of the input $\Sigma\Delta G^{\circ}_{un,i}$ and Σm_i). Note that when α_I is much lower than that of the other states, it is even possible to obtain a m′ value that is greater than Σm_i.

The effect of variation in the thermodynamic parameters on a three-state system is shown in Fig. 4. Although both $\Delta G^{\circ}_{un,i}$ and m_i values may vary, in these simulations we have only varied the m_i values and have fixed the $\Delta G^{\circ}_{un,1}$ and $\Delta G^{\circ}_{un,2}$ values to be symmetrical at 2.5 kcal mol^{-1}. The sum of the m_i values is still held at 5.0 kcal mol^{-1} M^{-1}, and m_1 is varied from 0 to 5.0 kcal mol^{-1} M^{-1}. The value of α_I is taken to be intermediate between that of α_N

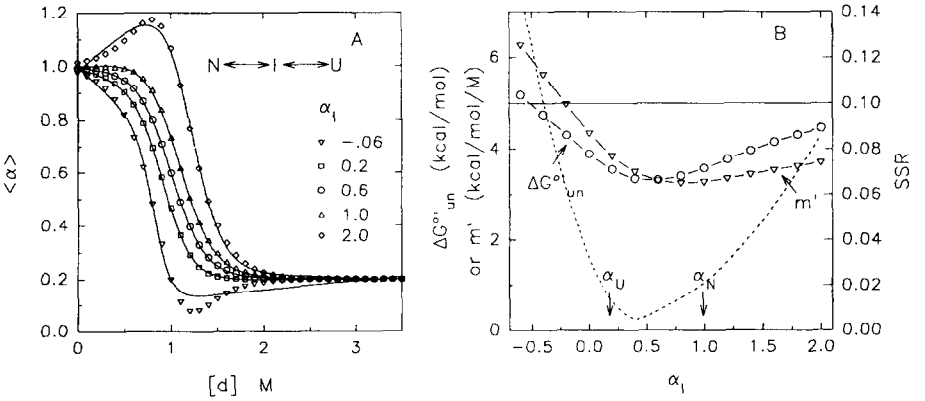

Fig. 3. Effect of varying the signal of the intermediate on the three-state system. (A) Plots of $\langle\alpha\rangle$ versus [**d**] for α_I values of −0.6, 0.2, 0.6, 1.0, and 2.0 (relative to $\alpha_N = 1.0$ and $\alpha_U = 0.2$). Simulated data is with $\Delta G^{\circ}_{un,1} = \Delta G^{\circ}_{un,2} = 2.5$ kcal mol^{-1} and $m_1 = m_2 = 2.5$ kcal mol^{-1} M^{-1} and with baseline slopes of zero. The solid lines are two-state fits to the simulated data. (B) Dependence of apparent ΔG°_{un} (○) and m' (▽) values on α_I. Shown as the dashed curve is the sum of the squares of the residuals for the fit to a two-state model.

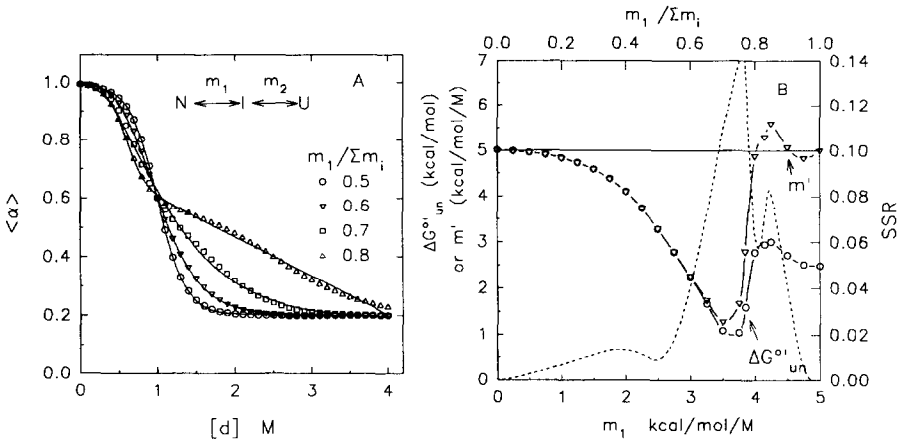

Fig. 4. Effect of varying the value of m_1 on a three-state transition. (A) Plots of $\langle \alpha \rangle$ versus **[d]** for $m_1/\Sigma m_i$ (where $\Sigma m_i = 5$ kcal mol^{-1} M^{-1}) values of 0.5, 0.6, 0.7, and 0.8. Simulated data is with $\Delta G^{\circ}_{un,1} = \Delta G^{\circ}_{un,2} = 2.5$ kcal mol^{-1}, $\alpha_N = 1.0$, $\alpha_I = 0.6$, and $\alpha_U = 0.2$ (baselines slopes of zero). The solid lines are two-state fits to the simulated data. (B) Dependence of apparent $\Delta G^{\circ\prime}_{un}$ (○) and m' (▽) values on $m_1/\Sigma m_i$ for fits to a two-state model with the assumption that the initial baseline is zero. If this pre-transition baseline is not fixed at zero, the apparent $\Delta G^{\circ\prime}_{un}$ and m' values will have a wider range. The dashed curve is the sum of the residuals squared for the two-state fit of the simulated data.

and α_U (the range found difficult to reveal in Fig. 3). The simulations in Fig. 4(A) show that a sigmoidal curve is found for $m_1/\Sigma m_i$ ratios less than about 0.6. At higher $m_1/\Sigma m_i$ the curves show the presence of a second transition. When $m_1/\Sigma m_i$ approaches 1.0, the curve is again sigmoidal (not shown). Fig. 4(B) shows the apparent $\Delta G^{\circ\prime}_{un}$ and m' that would be obtained from a fit with the two-state model. The trend is complicated. At $m_1/\Sigma m_i = 0$, the transition is actually a two-state N ⇌ U process, with recovered $\Delta G^{\circ\prime}_{un}$ and m' values being the full input values for going from N to U. As $m_1/\Sigma m_i$ increases to about 0.6, the maximum population of the I state increases, but the data will still be well described by a two-state fit (see the SSR in Fig. 4(B), shown as the dashed curve; values of SSR below about 0.04 for a two-state fit are judged to be acceptable). The apparent $\Delta G^{\circ\prime}_{un}$ and m' values will progressively decrease. The deviation from a two-state process becomes obvious in the range of $m_1/\Sigma m_i \approx 0.6$ to 0.9. The apparent $\Delta G^{\circ\prime}_{un}$ and m' values can take wide excursions in this range, due primarily to the tendency of the fitting program to liberally adjust the pre- and post-transition slopes in an attempt to fit the data to a two-state function. Actually, the fits shown are for the case in which the initial slopes in Fig. 4(a) are fixed as zero. Even a wider range for the apparent $\Delta G^{\circ\prime}_{un}$ and m' values (including negative values for $\Delta G^{\circ\prime}_{un}$ and values of m' that are 30% higher than Σm_i) occur when the pre-transition baseline slope is allowed to vary in the fit.

To summarize: (1) an apparently sigmoidal curve is expected for multi-state transitions for a variety of state energy levels, with the apparent (i.e. forced two-state fitted) $\Delta G^{\circ\prime}_{un}$ and m' values being less than the $\Sigma\Delta G^{\circ}_{un,i}$ and Σm_i; (2) an asymmetric type of multi-state model will yield apparent $\Delta G^{\circ\prime}_{un}$ values that are slightly below the true value for the first N ⇄ U_1 step; (3) the ability to determine deviations from a two-state fit is improved if the signal for the intermediate is much greater or lower than that of the N and final U states and/or if the stepwise thermodynamics are such as to give a relatively large maximum mole fraction of the intermediate state; and (4) values of m' greater than the Σm_i can be determined under certain conditions in a forced two-state fit. When attempting to interpret the thermodynamics of the denaturant-induced unfolding of a set of related proteins, each of these factors should be considered. Although we have used denaturant-induced unfolding in these simulations, similar arguments hold for unfolding induced by other perturbants (i.e. a multi-state transition can give an appar-

ent $\Delta H'_{un}$ that is smaller than the $\Sigma\Delta H_{un,i}$ or an apparent $\Delta V'_{un}$ that is smaller than the $\Sigma\Delta V_{un,i}$).

9. When do we have distinct U macrostates, versus a distribution of U microstates?

The above simulations, particularly that for an asymmetric five-state model, leads to the question of whether the U_1, U_2, U_3 etc., unfolded states are best considered to be separate macrostates, or whether they are better described as microstates of the same unfolded macrostate. This then returns to the first question of what is an unfolded thermodynamic state. For U_1, U_2, U_3 etc. to be macrostates, each should be separated by a free-energy barrier from the other macrostates and it should be possible to have transitions between any pair of such macrostates (i.e. $N \rightleftharpoons U_3$ or $U_1 \rightleftharpoons U_4$) with ΔG values that are additively related to all other ΔG values. Of course, it helps if a particular U_i state has a distinctive, resolved signal (e.g. a characteristic NMR peak), so that its population can be directly tracked.

If the free-energy barriers and $\Delta G_{i\rightarrow j}$ between such U_i and U_j states are small and the degree to which the free energy levels of the states varies with the perturbation axis (i.e. the $m_{i\rightarrow j}$ for denaturant unfolding or the $\Delta S_{i\rightarrow j}$ for thermal unfolding) is small, then it may be more realistic to describe these states as a distribution of microstates of the same overall macrostate. With a small $\Delta G_{i\rightarrow j}$ and small variations in $\Delta G_{i\rightarrow j}$ with perturbant, there will only be gradual, non-sigmoidal shifts in the population of unfolded species along the perturbant axis. For $\Delta G_{i\rightarrow j}$ and its variation with perturbant to be small, the unfolded species must have a similar solvent exposed surface area, which follows from the above arguments that the ΔSASA is the molecular coordinate that is correlated to the ΔC_p, ΔH, ΔS (and hence ΔG), and denaturant m for a particular $N \rightleftharpoons U_i$ transition. Of course, the distinction between multiple unfolded macrostates and a distribution of unfolded microstates becomes blurred when the free-energy changes (and the degree to which the free-energy changes vary with perturbant) between the unfolded species, whatever they are called, becomes small.

Consider the following description of the unfolding of a protein in terms of the existence of a distribution of microstates for the unfolded macrostate, which leads to the simulations in Fig. 5. This simulation is for denaturant-induced unfolding, using Eq. (2) for simplicity. The basis of this model is that microstates exist and that they have varying ΔSASA with respect to the N state. A typical 150 amino acid globular protein will have a ΔSASA of about 14 000 Å^2 for its unfolding to a fully extended, solvated structure. Since calculated ΔSASA are for such an extended unfolded structure, it is reasonable to assume that there will exist microstates that are less extended and thus have smaller ΔSASA. For simplicity we assume that the N state is a discrete species, and that the ΔSASA for unfolding can range from about 8000 to 17 000 Å^2. Further we assume that about 2/3 of this average total ΔSASA is due to exposure of apolar side chains and the remainder is due to exposure of polar groups. Using equations in the legend of Fig. 5 for the correlation between $\Delta SASA_{apolar}$ and $\Delta SASA_{polar}$ and ΔC_p, and values for the correlation constants from Freire and Murphy [22], we calculate ΔH_{un} and $\Delta S_{un,solv}$ for the unfolding of the microstates over the range of ΔSASA. The total ΔS_{un} is the sum of the solvation contribution plus a configurational contribution, $\Delta S_{un} = \Delta S_{un,solv} + \Delta S_{un,conf}$. Lee et al. [25] have argued that the latter can be calculated from consideration of the probability of side change conformers and the backbone entropy of the flexible unfolded state. If we are assuming a distribution of microstates, with varying extent of chain extension, then we would expect there to be a variation of the $\Delta S_{un,conf}$ across the distribution of U microstates, and that this variation of $\Delta S_{un,conf}$ will vary in a compensating manner with respect to that for the solvation contribution. That is, the more extended species will have larger, positive $\Delta S_{un,conf}$ contribution and larger negative $\Delta S_{un,solv}$ contribution. We arbitrarily assumed a variation of $\Delta S_{un,conf}$ across the ΔSASA axis to give a symmetrical distribution for the U microstates (at zero **[d]**). Shown in the Fig. 5(A) is this initial distribution of unfolded microstates and shown in Fig. 6 (top panel) are the thermodynamic parameters used in the simulation. Again, we have used established thermodynamic trends between ΔSASA and ΔC_p, ΔH_{un}, and $\Delta S_{un,solv}$, along with a reasonable estimate of $\Delta S_{un,conf}$, to generate the distribution of microstates,

with the only fundamental assumption being that a range of $\Delta SASA_i$ unfolded microstates is possible. The sharpness (width) of the initial distribution can be changed by altering the assumed dependence of $\Delta S_{un,conf,i}$ with $\Delta SASA_i$. What is obvious from Fig. 6, and what recalls the analysis of Kauzmann [6], is that the configurational entropy and solvation entropy terms dominate and compensate in determining the overall thermodynamics of protein stability.

The value of m_i for the individual microstates will also depend on their $\Delta SASA_i$, as argued by Schellman [29] and Tanford [7,8]. Here we use the linear correlation reported by Myers et al. [30] between m and $\Delta SASA$ to give an average value of m of 1.66 kcal mol^{-1} M^{-1} for the initial distribution of microstates (at [**d**] = 0). Since m increases along the $\Delta SASA$ axis, this model predicts that there will be a shift in the distribution to increasingly populate larger $\Delta SASA$ microstates as [**d**] is increased, as is shown in Fig. 5(B). This simulation shows the shift in distribution with increasing [**d**] that has been suggested by Dill and coworkers [10,77]. The simulations by Lumry et al. [1] showed the same type of shift in distribution of microstates of U with temperature as the perturbation axis, although their simulations did not directly relate the shape of the distribution and its shift to the $\Delta SASA$ for the various microstates. Such a shift will occur along the temperature axis, since the microstates that have the largest

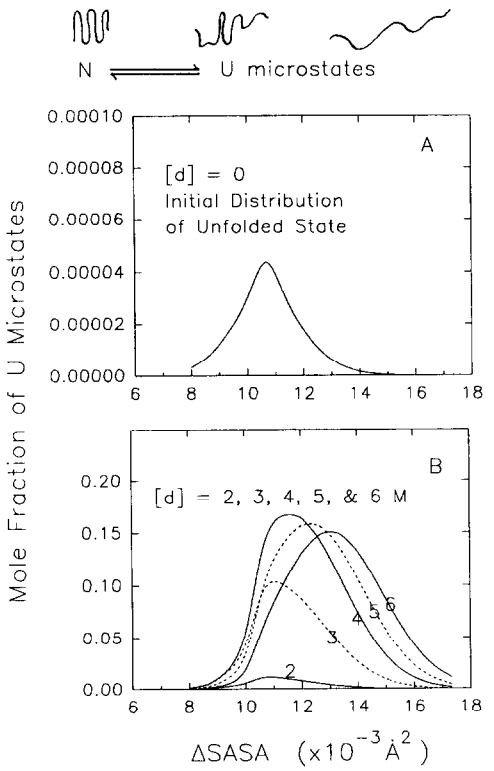

Fig. 5. Simulation of a distribution of microstates that can exist during the course of denaturant-induced unfolding of a protein. The initial distribution, shown in the top panel (A) (note expansion of the y axis), was calculated as follows. A range of microstates with varying $\Delta SASA_i$ is assumed. $\Delta SASA_{apolar}$ is allowed to range from 5600 to 10000 Å^2; the $\Delta SASA_{polar}$ is allowed to range from 2400 to 7000 Å^2, giving a range of total $\Delta SASA_i$ of 8000 to 17000 Å^2. The $\Delta C_{p,i}$ for a microstate is calculated as $\Delta C_{p,i} = 0.45 \cdot \Delta SASA_{apolar,i} - 0.26 \cdot \Delta SASA_{polar,i}$. The enthalpy change at 25 °C for the unfolding of each microstate is calculated as $\Delta H_{un,i} = 31.4 \cdot \Delta SASA_{polar,i} - 8.44 \cdot \Delta SASA_{apolar,i} + \Delta C_{p,i} \cdot (298 - T_R)$, where T_R is 333 K. The total entropy change, $\Delta S_{un,i}$, for the unfolding of $\Delta SASA_i$ species i at 25 °C is the sum of a solvation component, $\Delta S_{solv,i}$, plus a configurational entropy component, $\Delta S_{conf,i}$. The value of $\Delta S_{solv,i}$ is calculated as $\Delta S_{solv,i} = 0.45 \cdot \Delta SASA_{apolar,i} \cdot \ln(298/385) - 0.26 \cdot \Delta SASA_{polar,i} \cdot \ln(298/335)$. The configurational entropy component, $\Delta S_{conf,i}$, for the microstates were chosen to range from 0.57 to 1.28 kcal mol^{-1} K^{-1}, having a value of 0.784 kcal mol^{-1} K^{-1} (which corresponds to about 5.5 cal mol^{-1} K^{-1} $residue^{-1}$) at the center of the initial distribution. This $\Delta S_{conf,i}$, together with the above $\Delta S_{solv,i}$ and $\Delta H_{un,i}$, gives a free-energy change for unfolding, $\Delta G_{un,i} = \Delta H_{un,i} - T \cdot (\Delta S_{solv,i} + \Delta S_{conf,i})$. The minimum $\Delta G_{un,i}$ is 5.92 kcal mol^{-1}, a value that is reasonable for a protein having 150 amino acids. The mole fraction of a microstate is calcuated as $X_i = \exp(-\Delta G_{un,i}/RT)/(1 + \Sigma\exp(-\Delta G_{un,i}/RT))$, where the summation is from $i = 1$ to n microstates. To create an initial normal distribution, the value of the configurational entropy was allowed to vary with i in the following manner. The $\Delta S_{conf,i}$ was allowed to increase with increasing $\Delta SASA_i$, but the slope of this increase was greater below the desired center of the distribution and the slope with respect to $\Delta SASA_i$ was smaller for $\Delta SASA_i$ above the center. The values of the various thermodynamic parameters for each $\Delta SASA_i$ microstate are given in Fig. 6. (The constants used in the above simulation were taken from Refs. [22,28]). The variation of $\Delta G_{un,i}$ with $\Delta SASA_i$ results in the normal distribution shape in panel (A) for the initial unfolded state distribution in the absence of denaturant. The total mole fraction of the unfolded macrostate is only 1.6×10^{-4} in the absence of denaturant. The bottom panel shows the increase in the population of the unfolded microstates and the shift toward larger $\Delta SASA_i$ with the addition of denaturant (from 2 to 6 M). These simulations assumed that each of the above microstates has an m_i value given by $374 + 0.11 \cdot \Delta SASA_i$ (in cal mol^{-1} M^{-1}; correlation taken from Myers et al. [30]).

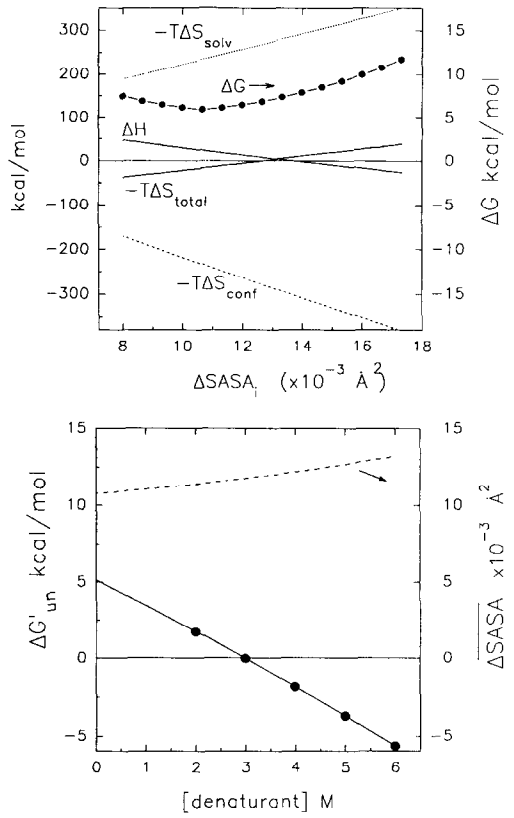

Fig. 6. The top panel shows the $\Delta G_{un,i}$ (expanded right axis), $\Delta H_{un,i}$, and $-T\cdot\Delta S_{un,i}$ versus $\Delta SASA_i$ used to create the initial distribution of unfolded microstates. Shown as dashed lines are the patterns for the $\Delta S_{solv,i}$ and $\Delta S_{conf,i}$ used in the simulation. The bottom panel shows the variation of the apparent ΔG_{un} and population average ΔSASA (right axis) with **[d]**, where the former is defined as $\Delta G_{un} = -RT\ln(\Sigma K_{un,i})$ and the latter is calculated as $\Delta SASA = \Sigma X_i \cdot \Delta SASA_i / \Sigma X_i$, where the summations are over all unfolded microstates. The plot of ΔG_{un} vs. **[d]** appears linear, though it is slightly curved; the intercept and slope give an apparent $\Delta G^{o'}_{un} = 5.29$ kcal mol^{-1} and an apparent $m' = 1.80$ kcal mol^{-1} M^{-1}, which can be compared to the actual (inputted) free energy change of 5.14 kcal mol^{-1} between N and all the U microstates (at **[d]** = 0) and $m = 1.66$ kcal mol^{-1} M^{-1} for the initial distribution of unfolded microstates. Note that the above definition of $K_{un} = \Sigma K_{un,i}$ includes the several nearly-degenerate unfolded microstates (i.e. $K_{un} = (\Sigma[U_i])/[N]$), so that the actual ΔG^{o}_{un} at **[d]** = 0 has a smaller value than the smallest $\Delta G^{o}_{un,i}$ for the most populated unfolded microstate.

ΔSASA, at the initial stage of thermal unfolding, will have the largest ΔC_p for solvation and hence the largest ΔH for unfolding.

10. How will such a distribution of microstates affect signals that track the conformational transitions?

If there is a distribution of microstates for U, a population-weighted average $\overline{\Delta SASA}$ for the distribution of U microstates can be imagined (and can be calculated for our simulation). This average $\overline{\Delta SASA}$ will increase with increasing **[d]** (or temperature), as the population is gradually shifted toward the more extended and solvent exposed microstates. If one is measuring the CD spectrum of the protein, then, following the large cooperative change in signal due to the transition from the N state to the initial distribution of U microstates, it is reasonable to expect a post-transition gradual change in the molar ellipticity that reflects a decrease in secondary structure as the distribution of unfolded chains expands further with an increase in the denaturing condition. With steady-state fluorescence it is a little more difficult to predict the effect of a gradual shift in the distribution of U microstates. The more expanded (larger $\Delta SASA_i$) microstates may provide less shielding of the tryptophan residues, but the incremental solvent exposure of the latter may not cause much of a change, unless the tryptophans have limited average accessibility in the initially formed U distribution. Also, thermally activated quenching processes will probably dominate the post-transition baseline for temperature studies. Fluorescence resonance energy transfer studies would be expected by this model to show a gradual increase in the distance between a donor and an acceptor attached at two sites within an unfolded protein. Studies by Brand et al. [78] suggest that such a post-transition gradual increase in donor–acceptor distance occurs for a *Staphylococcal* nuclease mutant as it is unfolded by guanidine–HCl.

Since the ΔC_p for thermal unfolding can be directly related to the ΔSASA for an unfolded microstate [40], it is expected that there will be a post-transition gradual increase in the average excess C_p for a protein due to the solvation effect, as the distribution shifts to larger ΔSASA microstates. The contribution of this shift to the total C_p of the protein may be small, however, compared to the dominant contribution from solvation, which has an intrinsic temperature dependence [31].

If there is a distribution of microstates for the U macrostate, what will be the effect of such a distribution on the apparent thermodynamic parameters that one would obtain by analysis of data that tracks the unfolding of a protein? Even if there are post-transition trends, due to the above distributional shifts or due to intrinsic changes in the signals by the perturbants, data for proteins almost always show that such baseline trends are sufficiently gradual that they appear linear (or at least modestly curved, so that a final baseline can be extrapolated). Pre-transitional baseline trends are usually a minor problem, unless the cold unfolding process begins to contribute and/or the protein is so unstable that the pre-transition region cannot be well defined. If both baseline trends are reasonably linear, then the ΔG°_{un} that one would obtain from denaturant-induced unfolding should be the value for the transition from the N state to the initial distribution of the U microstate (see the legend of Fig. 6, where the extrapolated ΔG°_{un} is compared to the value used in the simulation). This initial distribution of U microstates is in equilibrium with the N state at the reference conditions, making it the thermodynamically relevant ensemble of U. Likewise, the m value should be that for the transition from the N state to the initial U state. If, in a study of a series of mutant proteins, there are variations in the magnitude of the thermodynamic parameters among the set of proteins, this variation will probably have little to do with the relative extent to which the U distributions shift along the perturbation axis with increasing perturbant. Instead, differences in thermodynamic parameters must be related to differences in the N state, the initial U state and its distribution (i.e. where this distribution is along the ΔSASA coordinate), and whether the transition is being analyzed by a valid thermodynamic model (i.e. does the two-state model apply in all cases within a series?).

There should be a limit to the extent that the unfolded state can expand and also a limit to the extent that the signals can change. If a random flight coil has the highest chain entropy, then further stretching such a coil will lead to a decrease in the configurational entropy contribution; a polypeptide can only be stretched so far [10], even when being solvated by denaturant molecules or charged by protons. The spectroscopic measurements will also have boundaries. The fluorescence quantum yield of tryptophan in a protein cannot be negative and hardly ever has a value above 0.4; far UV CD signals in the 222 nm region are bounded at an upper limit for the mean residue ellipticity of about -40×10^3 deg cm^{-2} $dmol^{-1}$ for a completely helical polypeptide and approach zero as a protein unfolds, rarely giving positive ellipticities. Such "wall" effects could be a cause of non-linear baseline regions, although, as mentioned above, it is usually found that baseline regions are approximately linear.

11. Is the same unfolded state formed by unfolding along two different perturbation axes?

A growing number of research groups have taken the approach of studying the unfolding of a protein along more than one perturbation axis [37,63,79–86]. The logic is clear, but there are additional questions that are raised. The first question is whether one is forming the same U state by traveling along various perturbation axes. Some diametric answers have been given to this question. Tanford concluded that different unfolded states are produced using different unfolding agents [7]. In apparent contrast, others [31,34,37,40,87] have argued that heat, acid, urea and guanidine–HCl denatured states are a common thermodynamic macrostate. These two points of view depend, to a large measure, on whether one is focusing on structure versus thermodynamic state (Section 3). Proponents of the common unfolded macrostate have acknowledged that the distribution of microstates and average structure of the unfolded macrostate may differ with different perturbants. The above question is further complicated if one compares the unfolded protein at different distances along a pair of perturbation axes. The ΔG_{un} value for forming the U state (whether we view it as a distribution of microstates or a discrete state) at any extent of perturbation is a projection based on the pertinent equation relating ΔG_{un} to the perturbation axis. So the ΔG_{un} at $[\mathbf{d}] = 2$ M will differ from that at $[\mathbf{d}] = 3$ M, etc., even for the same denaturant; the relative depths of the free energy wells progressively change. In analyzing any type of unfolding data with equations in Table 1, we attempt to "extrapolate back" to obtain the ΔG°_{un} in the absence of the

perturbant. So the question should be whether the U state(s) (and/or their distributions) in the absence of different perturbants is/are the same. Once stated in this manner, the initial question can be addressed more clearly. If there are two different unfolded states, U_1 and U_2 (which may be separated by a large energy barrier), available to the protein in the absence of perturbant, then, in principle, it should make no difference what these "absent" perturbants are; the two unfolded states are hypothetically extant, although populated to a vanishingly small degree in the absence of either perturbant. Each of these U states may have its individual ΔG°_{un} value, which need not be the same for two U states.

Let us further speculate that one type of perturbation (call it $\mathbf{d}_1$) can lead to one unfolded state, U_1, by having a large m_1, and that the other perturbant (call it $\mathbf{d}_2$) can lead to U_2 by virtue of having a large m_2 (and we assume that the m_2 for $\mathbf{d}_1$ is zero and that the m_1 for $\mathbf{d}_2$ is zero, so that the two perturbants lead exclusively to a single U state) [5]. This amounts to a bifurcated type of model, with N being able to go exclusively to either the U_1 or U_2 state, depending on the presence of the particular perturbant. Unfolding by each type of perturbant could be a two-state process. Exclusive unfolding will result in a phase diagram such as that in Fig. 7(A) (solid line). What is noteworthy about this phase diagram is that the presence of pre-transition concentrations of one perturbant will have essentially no effect on the unfolding induced by the second perturbant. Further, when in the post-transition concentration range of $\mathbf{d}_1$, it will require higher concentrations of $\mathbf{d}_2$ to form the U_2 species (than would be the case in the absence of $\mathbf{d}_1$; presuming that the U_1 and U_2 species can be distinguished, e.g. by a method that resolves signals for each unfolded state); i.e. the two perturbants act competitively. Whereas the existence of two different U states may seem like a logical possibility, we know of no data which shows this type of competitive or anti-synergistic action of two denaturing agents [6].

Now consider that the $N \rightleftharpoons U_1$ and $N \rightleftharpoons U_2$ transitions are not exclusively induced by perturbants $\mathbf{d}_1$ and $\mathbf{d}_2$, respectively. That is, assume that $\mathbf{d}_1$ and $\mathbf{d}_2$ can also induce formation of states U_2 and U_1, respectively, but with m values that are half the magnitude of their "preferred" unfolded state. In this case there will be the commonly observed synergistic effect of two perturbants; the presence of low levels of $\mathbf{d}_2$ makes it easier to induce the $N \rightleftharpoons U_1$ transition by $\mathbf{d}_1$ and vice versa (see Fig. 7(A), dotted lines). Also it is important to note that this model predicts that the unfolding transitions will be a three-state process under some conditions. This is illustrated in Fig. 7(B), where simulations are shown for the $\mathbf{d}_1$ induced unfolding in the presence of different concentrations of $\mathbf{d}_2$. Also, note that equilibrium thermodynamic studies alone will not be able to distinguish such a bifurcated (or triangle) model from a linear three-state $N \rightleftharpoons U_1 \rightleftharpoons U_2$ model, an example phase diagram for which is shown in Fig. 7(C). The latter may also be considered to be a $N \rightleftharpoons I \rightleftharpoons U$ model, where I is an intermediate. The question of whether these U_1 and U_2 species (or I and U species) are actual macrostates versus a distribution of microstates leads us back to the essence of the first and second questions. What is a state? The answer will depend on whether a first-order cooperative transition between the two U states can be induced along one or more perturbation axes and whether the signals for the two U species are discernably different or resolved. Kinetics studies can also help answer the question through determination of whether or not there is a large free-energy barrier between the species.

For comparison we have also presented in Fig. 7(D) the phase diagrams expected if there is only a single U state that can be formed by the synergistic action of two different perturbants. The latter situa-

[5] As with the simulations in Fig. 2Fig. 3Fig. 4, we assume in the simulations that follow that the perturbation is by chemical denaturants and we use the LEM equation (Eq. (2)) to describe this perturbation. The arguments can also be applied to any other combination of perturbants, i.e. T and pH, or P and [**d**], with the corresponding functions in Table 1.

[6] This exclusive action of two different perturbants does apply to the case in which one perturbant is a specific ligand, which binds only to the native state, stablizing it by mass action as a binary complex, and the other perturbant is a denaturant, pH, or temperature.

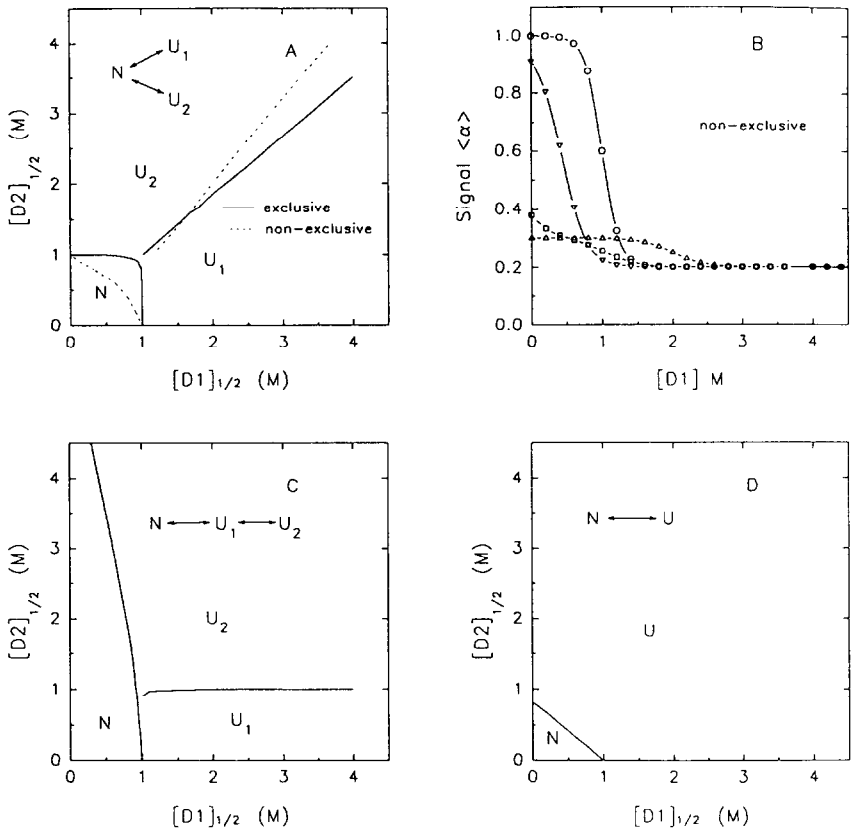

Fig. 7. Example phase diagrams for three possible unfolding models. (A) Exclusive formation of two different unfolded states, U_1 and U_2, by perturbation by the respective denaturants, $\mathbf{d_1}$ and $\mathbf{d_2}$. The solid lines between N and either U state is the condition for which $X_N = 0.5$. The line between U_1 and U_2 is for $X_{U1} = X_{U2}$. Simulated with $\Delta G^\circ_{N \rightarrow U1} = 6.0$ kcal mol^{-1}, $m_{d1,N \rightarrow U1} = 6.0$ kcal mol^{-1} K^{-1}, $\Delta G^\circ_{N \rightarrow U2} = 5.0$ kcal mol^{-1}, $m_{d2,N \rightarrow U2} = 5.0$ kcal mol^{-1} K^{-1}, with $m_{d1,N \rightarrow U2} = m_{d2,N \rightarrow U1} = 0$. The dashed lines are for non-exclusive, but preferential, unfolding by the respective denaturants, with the m values for $\mathbf{d_1}$ inducing unfolding to U_2 and $\mathbf{d_2}$ inducing unfolding to U_1 being 1/2 of that for their preferred product. (B) Plots of $\langle \alpha \rangle$ versus $[\mathbf{d_1}]$ expected for the non-exclusive unfolding model in panel (A), for the presence of $[\mathbf{d_2}] = 0$ (○), 0.8 (▽), 1.2 (□), and 2.0 M (△). It is assumed that $\alpha_N = 1$, $\alpha_{U1} = 0.2$, and $\alpha_{U2} = 0.3$. Note that at around $[\mathbf{d_2}] = 1$ the unfolding profile will no longer be sigmoidal, and that at high concentrations of $\mathbf{d_2}$, the addition of $\mathbf{d_1}$ will induce the transition from U_2 to U_1. (C) Three-state sequential model, with $\mathbf{d_1}$ inducing the unfolding of N to U_1 and with $\mathbf{d_2}$ only being able to induce the unfolding of U_1 to U_2, with the following parameters: $\Delta G^\circ_{N \rightarrow U1} = 5.0$ kcal mol^{-1}, $m_{d1,N \rightarrow U1} = 5.0$ kcal mol^{-1} K^{-1}, $\Delta G^\circ_{U1 \rightarrow U2} = 1.0$ kcal mol^{-1}, and $m_{d2,U1 \rightarrow U2} = 1.0$ kcal mol^{-1} K^{-1}. (D) Two-state model in which both $\mathbf{d_1}$ and $\mathbf{d_2}$ induce formation of the same unfolded state, with $\Delta G^\circ_{N \rightarrow U} = 5.0$ kcal mol^{-1} and $m_{d1} = 5.0$ kcal mol^{-1} K^{-1} and $m_{d2} = 6.0$ kcal mol^{-1} K^{-1}.

tion may seem trivial, but it leads to the following two important tests or applications of the two-state thermodynamic model: (1) different perturbants should yield the same ΔG°_{un}, and (2) the action of any number of perturbants is additive, with respect to their effect on the ΔG_{un} for an unfolding transition. A number of studies have attempted to compare the ΔG°_{un} for two denaturants, usually urea and guanidine–HCl, for a given protein. In many cases agreement is found, in support of the two-state model with a common U macrostate. There have been several examples in which the ΔG°_{un} for urea and guanidine–HCl do not agree within the uncertainty of the extrapolated ΔG°_{un} values [37,79,88]. Assuming that these differences are not a consequence of the failure of the LEM model (i.e. due to a non-linear relationship between ΔG_{un} and [**d**], particularly for guanidine–HCl), these discrepancies in ΔG°_{un} can mean

that :(1) there are two different U macrostates that are exclusively or selectively populated by the two different denaturants; (2) that the transition is actually multi-state, resulting in underestimates of the cumulative ΔG°_{un} for both denaturants when data are incorrectly analyzed as being two state; and (3) that one or both of the denaturants is interacting in a secondary manner, with either the N or U state, such that the equations in Table 1 do not completely describe the interactions. An obvious chemical difference between urea and guanidine–HCl is that the latter is a salt. Monera et al. [88] have clearly shown that guanidine–HCl gives different apparent ΔG°_{un} and m values, as compared to those for urea, for the unfolding of a set of four coiled-coil model proteins engineered to have electrostatic interactions ranging from 20 attractions to 20 repulsions. Presumably, uncharged urea gives the more valid determination of ΔG°_{un}. Guanidine–HCl, by being a salt, is able to shield electrostatic repulsions within the folded protein and weaken attractions, thus giving an altered determination of ΔG°_{un} when such interactions are present. Similarly, Yao and Bolen [37] and Pace et al. [79] have shown that the discrepancies between the ΔG°_{un} for guanidine–HCl and urea-induced unfolding of ribonuclease A and T_1 can be attributed to the former denaturant's stabilizing interaction with the native state of these proteins. Each study reached the conclusion that the primary explanation for the discrepancies in ΔG°_{un} was not due to a breakdown in the basic two-state model, but was due to an interaction of guanidine–HCl with the native state [89,90].

To model the expected consequence of such an interaction between a denaturant and the native state, consider the simulation in Fig. 8. Here, in addition to its action as a denaturant (following the LEM equation), we have assumed that there is a single binding site for a denaturant molecule on the native protein, to form a N · d species, for which the signal is assumed to be unchanged from that of N. Shown are simulations in which the association constant for denaturant, K_d, is allowed to vary from 0 to 1000 M^{-1}. As seen, in Fig. 8(A), the transition profile shifts to higher **[d]**, as K_d is allowed to increase. The apparent ΔG°_{un}, recovered from a forced two-state fit, increases with increasing K_d (Fig. 8(B)), as expected. What is less obvious is that the apparent value of m', which would be obtained by fitting data to the two-state model, drops by about 10%, when K_d has a value of about 10 M^{-1}. A value of K_d of $\approx$ 10 M^{-1} does not seem unreasonable for the binding of guanidine–HCl to a native protein (and note that the simulation is for a single binding site; a similar effect would result with a smaller K_d and a larger number of binding sites), in view of the average association of 0.5–1 M^{-1} that have been determined for the binding of guanidine–HCl to native and unfolded proteins [40].

The second consequence of having a common

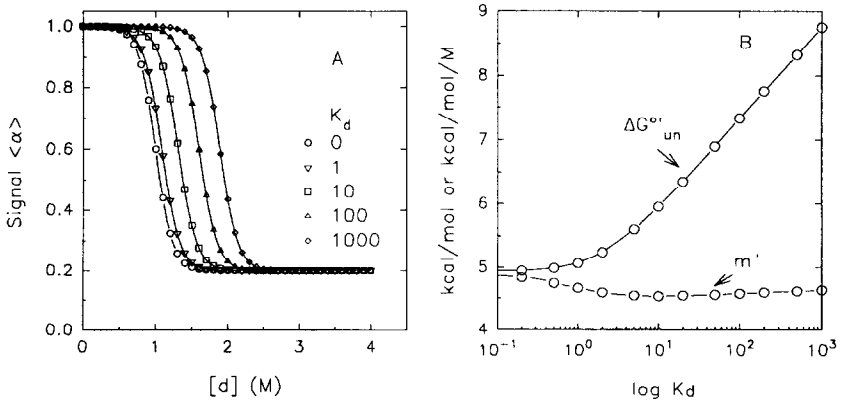

Fig. 8. Simulated effect of a model in which the denaturant is able to bind to a single site on the native state, thus stabilizing the protein before unfolding it. Simulations are with $\Delta G^{\circ}_{un} = 5.0$ kcal mol^{-1}, $m = 5.0$ kcal mol^{-1} K^{-1}, $\alpha_N = \alpha_{N \cdot d} = 1.0$, $\alpha_U = 0.2$. (A) Average signal versus **[d]** for various assumed values for the denaturant association constant, K_d. (B) Apparent ΔG°_{un} and m' values derived from two-state fits of data, as a function of the denaturant association constant.

unfolded macrostate for various perturbants, is that, in principle, one can consider a composite relationship that combines all of the relationships in Table 1, which would then provide a multi-dimensional function to describe the free energy surface along multiple perturbation axes. That is, the overall free energy change for the conformational transition would then be given as follows

$$\Delta G_{un}(T,P,\boldsymbol{d}_i,\mathrm{pH},x) = \Delta G^{\circ}_{un} + f(T) + f(P) + \Sigma f(\boldsymbol{d}_i) + f(\mathrm{pH}) + \Sigma f(x_i) \quad (9)$$

where the $f(...)$ values are functions that describe the change in free energy due to the respective type of perturbation, and x is any additional type of perturbation not discussed, such as the binding of a specific ligand to either the N or U state. (Note that f(pH) is also a function of temperature, and the other functions may be as well.) This type of equation is the basis for the above-mentioned comparison of ΔG°_{un} obtained with two or more different perturbants; if a similar ΔG°_{un} is obtained with different perturbants, this is support for the underlying assumption that the transition being investigated is two state.

In work in our lab we have collected data for the unfolding of *Staphylococcal* nuclease as induced by temperature, urea, pH, and pressure and we find that, to a first approximation, this composite relationship for the two-state model provides a good fit to the multi-dimensional data [47,86].

The extension of unfolding studies to multiple dimensions introduces questions about higher order terms, such as $\delta m/\delta T$, $\delta m/\delta$pH, $\delta\Delta H/\delta$[**d**], and $\delta\Delta V/\delta$pH, to mention a few. Whether or not these higher order terms are zero, or have positive or negative values, has been studied by different laboratories [63,79,83,85,86,91]. It is reasonable, we believe, to expect that most of these higher order terms are not zero. If so, we would not view this as indicating a failure of the two-state model, but as revealing the finer thermodynamic features of the protein folding problem.

12. Concluding remarks

The Gibbs Conferences have been marked by lively discussions of what we do and do not know about the thermodynamics of protein unfolding. There is no doubt that our understanding grows, but uncertainties persist. They keep us intrigued and they stimulate us to do experiments The important questions are not new and the answers are not necessarily simple or unique. We imagine that with time and energy these answers too will unfold.

Acknowledgements

This research was supported by NSF grant MCB 94-07167.

References

[1] R. Lumry, R. Biltonen and J.F. Brandts, Biopolymers, 4 (1966) 917–944.
[2] K.A. Dill, Biochemistry, 29 (1990) 7133–7155.
[3] H. Wu, Chin. J. Physiol., V (1931) 321–344; see also the revised version of this article, Adv. Protein Chem., 46 (1995) 6–26.
[4] M.A. Eisenberg and G.W. Schwert, J. Gen. Physiol., 34 (1951) 383–406.
[5] J.A. Schellman, Comp. Rend. Trav. Carlsberg Lab. Ser. Chim., 15 (1955) 230–259.
[6] W. Kauzmann, Adv. Protein Chem., 14 (1959) 1–63.
[7] C. Tanford, Adv. Protein. Chem., 23 (1968) 121–282.
[8] C. Tanford, Adv. Protein Chem., 24 (1970) 1–95.
[9] C.B. Anfinsen, Science, 181 (1973) 223–230.
[10] K.A. Dill and D. Shortle, Ann. Rev. Biochem., 60 (1991) 795–825.
[11] K.C. Aune, A. Salahuddin, M.H. Zarlengo and C. Tanford, J. Biol. Chem., 242 (1967) 4486–4489.
[12] T.R. Sosnick and J. Trewhella, Biochemistry, 31 (1992) 8329–8335.
[13] S. Seshadri, K.A. Oberg and A.L. Fink, Biochemistry, 33 (1994) 1351–1355.
[14] B.E. Bowler, A. Dong and W.S. Caughey, Biochemistry, 33 (1994) 2402–2408.
[15] Y. Goto, N. Takahashi and A.L. Fink, Biochemistry, 29 (1990) 3480–3488.
[16] A.L. Fink, L.J. Calciano, Y. Goto, T. Kurotsu and D.R. Pallerso, Biochemistry, 33 (1994) 12504–12511.
[17] S. Karplus, G.H. Snyder and B.D. Sykes, Biochemistry, 12 (1973) 1323–1329.
[18] A. Bierzynski and R.L. Baldwin, J. Mol. Biol., 162 (1982) 173–186.
[19] B. Lee and F.M. Richards, J. Mol. Biol., 55 (1971) 379–400.
[20] M.L. Connolly, J. Appl. Crystallogr., 16 (1983) 548–558.
[21] T.P. Creamer, R. Srinivasan and G.D. Rose, Biochemistry, 34 (1995) 16245–16250.

[22] K.P. Murphy and E. Freire, Adv. Protein Chem., 43 (1992) 313–361; E. Freire and K.P. Murphy, J. Mol. Biol., 222 (1991) 687–698.
[23] J.R. Livingstone, R. Spolar and M.T. Record, Biochemistry, 30 (1991) 4237–4244; R.S. Spolar, J.R. Livingstone and M.T. Record, Biochemistry, 31 (1992) 3947–3955.
[24] G. Nemethy, S.J. Leach and H.A. Scheraga, J. Phys. Chem., 70 (1996) 998–1004.
[25] K.H. Lee, D. Xie, E. Freire and M.L. Amzel, Proteins: Struct. Funct. Genetics, 20 (1994) 68–84.
[26] G.I. Makhatadze and P.L. Privalov, Protein Sci., 5 (1996) 507–510.
[27] D. Xie, R. Fox and E. Freire, Protein Sci., 3 (1994) 2175–2184.
[28] E. Freire, Annu. Rev. Biophys. Biomol. Struct., 24 (1995) 141–165.
[29] J.A. Schellman, Biopolymers, 17 (1978) 1305–1322.
[30] J.K. Myers, C.N. Pace and J.M. Scholtz, Protein Sci., 4 (1995) 2138–2148.
[31] P.L. Privalov and G.I. Makhatadze, J. Mol. Biol., 213 (1990) 385–391.
[32] F. Franks, R.H.M. Hatley and H.L. Friedman, Biophys. Chem., 31 (1988) 307–315.
[33] W.J. Becktel and J.A. Schellman, Biopolymers, 26 (1987) 1859–1876.
[34] P.L. Privalov and S.J. Gill, Adv. Protein Chem., 39 (1988) 191–234; P.L. Privalov, Ann. Rev. Biophys. Biophys. Chem., 18 (1989) 47–69.
[35] M.M. Santoro and D.W. Bolen, Biochemistry, 27 (1988) 8063–8068.
[36] M.M. Santoro and D.W. Bolen, Biochemistry, 31 (1992) 4901–4907.
[37] M. Yao and D.W. Bolen, Biochemistry, 34 (1995) 3771–3781.
[38] C.N. Pace, Methods Enzymol., 131 (1986) 226–280.
[39] K. Aune and C. Tanford, Biochemistry, 8 (1969) 4586–4590.
[40] G.I. Makhatadze and P.L. Privalov, J. Mol. Biol., 226 (1992) 491–505.
[41] R.A. Staniforth, S.G. Burston, C.J. Smith, G.S. Jackson, I.G. Badcoe, T. Atkinson, J.J. Holbrook and A.R. Clarke, Biochemistry, 32 (1993) 3842–3851.
[42] C.N. Pace and K.E. Vanderburg, Biochemistry, 18 (1979) 288–292.
[43] L.M. Mayr and F.X. Schmid, Biochemistry, 32 (1993) 7994–7998.
[44] J.F. Brandts, R.J. Oliveira and C. Westort, Biochemistry, 9 (1970) 1038–1047.
[45] S.A. Hawley, Biochemistry, 10 (1971) 2436–2442.
[46] C.A. Royer, A.P. Hinckl, S.N. Loh, K.E. Prehoda, X. Peng, J. Jonas and J.L. Markley, Biochemistry, 32 (1993) 5222–5232.
[47] M.R. Eftink and G.D. Ramsay, in J.L. Markley, D.B. Northrop and C.A. Royes (Eds.), High Pressure Effects in Molecular Biophysics and Enzymology, Oxford University Press, 1996, pp. 62–73.
[48] G.D. Ramsay and M.R. Eftink, Methods Enzymol., 240 (1994) 615–645.
[49] G. Ramsay, R.M. Ionescu and M.R. Eftink, Biophys. J., 69 (1995) 701–707.
[50] M.R. Eftink, Biophys. J., 66 (1994) 482–501.
[51] E.P. Kirby and R.F. Steiner, J. Phys. Chem., 74 (1970) 4480–4490.
[52] F.X. Schmid, in T.E. Creighton (ed.), Protein Structure: A Practical Approach, IRL Press, Oxford, 1989, pp. 251–285.
[53] M.R. Eftink, Methods Biochem. Anal., 35 (1991) 127–205.
[54] M. Shinitzky and R. Goldman, Eur. J. Biochem., 3 (1967) 139–144.
[55] R. Loewenthal, J. Sancho and A. Fersht, Biochemistry, 30 (1991) 6775–6779.
[56] M.E. Holtzer and A. Holtzer, Biopolymers, 32 (1992) 205–214.
[57] M.L. Tiffany and S. Krimm, Biopolymers, 12 (1973) 575–587.
[58] R. Woody, Adv. Biophys. Chem., 2 (1992) 37–79.
[59] M.L. Johnson and S.G. Fraiser, Methods Enzymol., 117 (1985) 301–342.
[60] D.A. Egan, T.M. Logan, H. Liang, E. Matayoshi, S.W. Fesik and T.F. Holzman, Biochemistry, 32 (1993) 1920–1927.
[61] S.D. Hoeltzli and C. Frieden, Biochemistry, 33 (1994) 5502–5509.
[62] J. Zhang, X. Peng, A. Jonas and J. Jonas, Biochemistry, 34 (1995) 8631–8641.
[63] G.S. Huang and T. Oas, Biochemistry, 35 (1996) 6173–6180.
[64] M.R. Eftink, I. Gryczynski, W. Wiczk, G. Laczko and J.R. Lakowicz, Biochemistry, 30 (1991) 8945–8953.
[65] B.K. Szpikowska, J.M. Beechem, M.A. Sherman and M.T. Mas, Biochemistry, 33 (1994) 2217–2225.
[66] D. Amir, S. Krausz and E. Haas, Proteins: Struct. Func. Genetics, 13 (1992) 162–173.
[67] R.S. Ruth, A.S. Cohen and B.L. Karger, Anal. Chem., 63 (1991) 1346–1350.
[68] V.J. Hilser, G. Worosila and E. Freire, Anal. Biochem., 208 (1993) 125–131.
[69] V.N. Uversky, Biochemistry, 32 (1993) 13288–13298.
[70] R.J.T. Corbett and R.S. Roche, Biochemistry, 23 (1984) 1888–1295.
[71] W. Shalongo, M.V. Jagannadham, P. Heid and E. Stellwagen, Biochemistry, 31 (1992) 11390–11396.
[72] T.E. Creighton, J. Mol. Biol., 129 (1979) 235–264.
[73] H. Fabian, C. Schultz, J. Backmann, U. Hahn, W. Saenger, H.H. Mantsch and D. Naumann, Biochemistry, 33 (1994) 10725–10730.
[74] I.H.M. van Stokkum, H. Linsdell, J.M. Hadden, P.I. Haris, D. Chapman and M. Bloemendal, Biochemistry, 34 (1995) 10508–10518.
[75] M. Kataoka, Y. Hagihara, K. Mihara and Y. Goto, J. Mol. Biol., 229 (1993) 591–596.
[76] E.E. Lattman, Curr. Opinion Struct. Biol., 4 (1994) 87–92.
[77] E. Shortle and A.K. Meeker, Proteins: Struct. Funct. Genetics, 1 (1986) 81–89.
[78] E. James, P.G. Wu, W. Stites and L. Brand, Biochemistry, 31 (1992) 10217–10225.
[79] C.N. Pace, D.V. Laurents and J.A. Thomson, Biochemistry, 29 (1990) 2564–2572.

[80] I. Plaza del Pino, C.N. Pace and E. Freire, Biochemistry, 31 (1992) 11196–11202.
[81] D. Barrick and R.L. Baldwin, Biochemistry, 32 (1993) 3790–3796.
[82] M. Straume, Methods Enzymol., 240 (1994) 530–568.
[83] C.M. Johnson and A.R. Fersht, Biochemistry, 34 (1995) 6795–6804.
[84] V.R. Agashe and J.B. Udgaonkar, Biochemistry, 34 (1995) 3286–3299.
[85] E.M. Nicholson and J.M. Stoltz, Biochemistry, 35 (1996) 11369–11378.
[86] R.M. Ionescu and M.R. Eftink, Biochemistry, in press.
[87] B. Chen and J.A. Schellman, Biochemistry, 28 (1989) 685–691.
[88] O.D. Monera, C.M. Kay and R.S. Hodges, Protein Sci., 3 (1994) 1984–1991.
[89] T.Y. Tsong, Biochemistry, 14 (1975) 1542–1547.
[90] Y. Hagihara, S. Aimoto, A.L. Fink and Y. Goto, J. Mol. Biol., 231 (1993) 180–188.
[91] J.H. Carra, E.A. Anderson and P.L. Privalov, Protein Sci., 3 (1994) 944–951.